Journal Home Page: https://sjes.univsul.edu.iq/

Effect of Nano-Silica on Geotechnical Properties and Microstructural Analysis of a Soft Soil

Gulistan Mohammed Ali [1, a,*]
Yousif Ismael Mawlood [2, a]

[a] Civil Engineering Department, Engineering College, Salahaddin University-Erbil, KR, Iraq

Article Information

Article History:
Received: April 13, 2026
Accepted: May 13, 2026
Available online: August , 2026

Keywords:
Soft soil; Nano-Silica; Soil Improvement; Geotechnical Properties; Microstructural analysis.

About the Authors:
Corresponding author:
Gulistan Mohammed Ali
E-mail: gulistan.ali@su.edu.krd
Researcher Involved:
Prof. Dr. Yousif Ismael Mawlood
E-mail: yousif.mawlood@su.edu.krd

DOI https://doi.org/10.17656/sjes.10214

Abstract

Nanotechnology offers an innovative approach to soil stabilization in geotechnical engineering. This study investigates the physical, mechanical, and hydraulic properties of soils treated with nano-silica at contents of 0%, 0.6%, 1.2%, 1.8%, 2.4%, and 3% by dry mass of the soil. Specimens for unconfined compressive strength (UCS) and permeability were compacted using a remolding device. The novelty of this study lies in the use of nanomaterials, which are rarely used in soil stabilization, and in employing a field-emission scanning electron microscope (FESEM) for microstructural analysis and to assess the effect of the curing period. Introducing 0.6% nano-silica reduced the liquid limit (LL) and plastic index (PI) by 13% and 53%, respectively. At curing periods of 1, 7, and 28 days, UCS and elastic modulus (E_{50}) increased by 208%-181.74%, 182.39%-108.75%, and 184.38%-188.41%, respectively, for 0.6% nano-silica. Furthermore, permeability decreased sharply at 0.6%, then increased at higher contents. FESEM analysis confirmed particle rearrangement and gel formation, thereby refining pores and enhancing strength. Furthermore, the average pore diameter decreased by nearly 32% with the addition of 0.6% nano-silica. However, excessive nano-silica led to agglomeration, resulting in unfavorable engineering properties. Eventually, nano-silica enhances MH soil physically, mechanically, and microstructurally. In addition, identifying 0.6% as the optimal content ensures cost-effective stabilization. Therefore, this study emphasizes the practical use of nano-silica in engineering projects, particularly for hydraulic barriers, landfill liners, and embankments.

1. Introduction

Fine-grained soils are characterized by their low bearing capacity and are susceptible to various types of geotechnical failures. High plasticity silt is characterized by a low coefficient of permeability, is often considered suitable for use in the construction of core of dams and landfill liners [1]. However, such soil remain vulnerable in terms of strength and serviceability requirements [2]. The traditional stabilizing materials, such as cement and fibers, can enhance strength; on the other hand, they often have the drawback of reducing permeability, which may negatively affect the hydraulic performance [3, 4]. Nanotechnology is an innovative approach for soil stabilization in geotechnical engineering. Nanomaterials are defined by particle dimensions smaller than 100nm in at least one direction. Essentially, in addition, the nanomaterials defined by the smaller the size, the higher the specific surface area. As a result, the nano-silica characteristics enable the refinement of soil pore structure, improvement of particle bonding, enhancement of strength and stiffness, and reduction in the permeability [5-8]. Consequently, the use of nanomaterials represents a new pathway for obtaining sustainable and efficient ground improvement.Changizi and Haddad [6] carried out a series tests on the high plasticity clay CH and found that the addition of nano-silica causes a reduction in liquid limit LL and shrinkage limit SL and increasing plastic limit PL. In addition, they reported that addition of 0.7% of nano-silica increases the unconfined compressive strength UCS nearly 156% in comparison with untreated soil sample. While, they reported that the elastic modulus were increased by means of 184% by adding 1% of nano-silica to the CH soil sample. Gu, Cai [9] investigated the impact of nano-silica on clayey soil. UCS of soil-nano-silica was increased from 200kPa to 600kPa by adding 2% nano-silica. In addition, UCS for cured samples of 28 days curing of 2% nano-silica was promoted from 1300kPa to 3000kPa. They reported the increase in brittleness and reduction in failure strain as well. Furthermore, they examined that nano-silica had less impact on soil pH value. Lu, Yao [10] conducted UCS of low plasticity clay CL under retaining the total mass of nano-silica and cement at 18% of dry mass of the soil and manipulating water-blinder ratio at 0.5 and 3%. Cube blocks with length of 70.7mm length were used for UCS test. UCS of cemented soil with 4% nano-silica at curing periods of 14days, 28days and 60days were increased by 47.07%, 40.45% and 40.38%. Chen, Ji [11]investigated the effect of nano-silica and polypropylene fiber PF on sandy clay. Incorporating 2% nano-silica and PF increased UCS nearly by 88% and 474%. Moreover, 2% nano-silica blended with 2% PF increased UCS by about 607%. The addition of nano-silica with PF produced a synergetic increase in UCS. Several authors reported that nanomaterials had a great role in immobilizing heavy metals and they were considered as environmentally friendly [12-14]. Thoroughly, the geotechnical engineering properties of the different types of soils were improved by different types of nanomaterials at the optimum level of the nanomaterials [8, 15-20].

Previous studies mostly tested nano-silica at 100% of the MDD and OMC and 90% of the MDD on the dry side of OMC [6, 9, 11, 21]. Traditional stabilizers like cement, lime, and fibers are limited in use due to increasing permeability. The pore size distribution was analyzed by the authors using nuclear magnetic resonance instead of FESEM [10, 11]. Mostly, soil-nano-silica specimens were examined and compacted at 100% of MDD and OMC. Furthermore, the effect of wet-side compaction of soil-nano-silica has not been systematically addressed. The role of nano-silica in MH soil has rarely been investigated. In addition, the pore size distribution via FESEM has not been explored. The novelty of the present work lies in compacting MH specimens on the wet side of the OMC point, systematically evaluating their engineering properties and microstructural outcomes, and pore size distribution using FESEM, which are rarely used in soil stabilization. This method demonstrates the role of nano-silica in mitigating moisture-induced strength loss, thereby addressing a critical gap in soil stabilization studies.

2. Location of Study Area

Dwin dam site, located near the historical Dwin castle, lies to the north of Erbil city in the Kurdistan Region of Iraq (Figure 1). Dwin soil sampling point was recorded in UTM zone 38S at 444400 mE and 4,041,800 mN.

3. Materials

The soil was excavated at the designated sampling point. Then, the disturbed soil samples were collected at depths of 1m and 6m below the ground surface. The particle size distribution of the soil is shown in Figure 2. The percentages of sand, silt and clay were 0.3, 55 and 43%, respectively. The soil was silt-dominant and had a reddish color. Furthermore, the soil was classified as high plasticity silt MH according to the Unified Soil Classification System (USCS). The maximum dry density (MDD) and optimum moisture content (OMC), obtained from standard proctor compaction curve, were 14.48 KN/m3 and 24.7%, respectively (Figure 3). This soil exhibits poor compaction characteristics, which pose significant challenges for its utilization in engineering projects. In this study, the nano-silica was used to assess the engineering properties of the soil samples. Figure 4 presents a scanning electron microscope (SEM) image of the SiO_2 nanoparticles. The nano silica appeared as white powder with a purity of 99.8%, and had a specific surface area SSA ranging between 150-200 m^2/g. in addition, the average grain size of the nanoparticles was 30 nm. Moreover, the surface properties of the nanoparticles were hydrophilic, with a pH value ranging between 7-8. Loss on ignition at 950°C for 2 hours was found to be ≤ 6%. Heavy metal content was also assessed with arsenic (As) ≤ 1ppm, lead (Pb) ≤ 1ppm and mercury (Hg) ≤ 1ppm. Chemical Abstracts Service (CAS) number of nano-silica is 112945-525.

4. Methods

4.1. Chemical Analysis of the Dwin Soft Soil

The chemical compositions of the soil sample were analyzed using X-ray fluorescence XRF with a benchtop spectrometer (Oxford Instruments X-supreme) as shown in Figure 5. The soil has sieved through sieve No. 200 and air-dried.

4.2. Sample Preparation

This study focusses on the physical, mechanical and hydraulic properties of soil specimens by adding nano-silica. Nano-SiO_2 was introduced into the soil at proportions of 0%, 0.6%, 1.2%, 1.8%, 2.4% and 3% by dry mass of the soil. The mixing process was carried out using mechanical mixer, and an addition of 0.5% was added to the target water content to compensate losses (ASTM D3551-08).

4.2.1. Index properties

Specific gravity G_s of the soil-nano-silica mixtures was determined in accordance with ASTM D854-02. The reported G_s values represent the oven-dry condition of the soil-nano-silica mixtures, independent of curing conditions. The Atterberg limits were determined following ASTM D4318-17. The soil was air-dried. Each portion of nano-SiO_2 was added to the soil and then mixed thoroughly until no traces of the nanoparticles remained.

4.2.2. Mechanical properties of the soil

UCS specimens were compacted at 95% of MDD (13.76 KN/m^3) on wet side of OMC (32.5%). Initial attempts with a rigid mold failed during extrusion, so a split mold was used, remolding specimens without deterioration (Figure 6a and b). The specimens, 50mm in diameter and 114mm in height, were compacted in three equal layers using static remolding device (Figure 6b). Afterwards, the specimens were sealed with plastic wrap and stored in an isolated foamed container with silica gel pads to maintain the moisture. Testing was conducted at a strain rate of 1.14 mm/min until failure at 20% of the strain reached (ASTM D2166). Figure 7 shows the UCS testing system.

4.2.3. Coefficient of Permeability

The permeability test was conducted in accordance with ASTM D5856-15. The soil specimens, 101.66mm in diameter and 102 mm in height, were compacted in three layers inside the permeameter mold at a unit weight of 13.76 KN/m^3 and moisture content of 32.5% (Figure 8a). Filter papers and porous stones were placed at the top and bottom of the soil sample. Afterwards, were placed at the top and bottom of the specimen before assembling the permeameter device. Nano-SiO_2 was incorporated at 0.6, 1.8, and 3%. The setup of the falling head permeability testing system is shown in Figure 8.

5. Results and Discussions

5.1. XRF Results

The results of chemical compounds are presented in Table 1. It shows that the soil contains 28.32, 18.67, 1.761, 1.04 and 0.27% of SiO_2, CaO, Al_2O_3, SO_3 and Na_2O, respectively. Existence of Na_2O obtains hydroxide for hydration process. In addition, presence of SiO2, CaO and Al2O3 contribute in formation of gelling products like columnar calcium alumina Aft, calcium aluminate hydrate C-S-H and calcium silicate hydrate C-S-H [22]. The detection of chemical components is helpful for explaining the strength gain of the treated soil samples, which are responsible for cementitious products between soil particles, and improving the engineering properties of the soft soil samples.

5.2. Index Properties

Table 2 shows the values of G_s of the soil samples by adding different percentages of nano-SiO_2. The monotonic increase in G_s value was confirmed. The neutral pH (7-8) of the nano-silica plays a key role in controlling particle dispersion which promotes stable and uniform distribution of nano-silica within the soil matrix. This improved dispersion refines pore filling and contributes to a denser soil structure. This microstructural enhancement is reflected in the measured increase in G_s. The increase of G_s values monotonically was confirmed by Al-Khazzaz, Aldaood [23].Table 3 presents the results of Atterberg limits: liquid limit (LL), plastic limit (PL), plasticity index (PI) and plasticity of the soil-nano-silica samples with different percentages of nano-silica. The LL had a lower value when 0.6% of nano-silica was introduced into the soil. The reduction was of approximately 13%. Reducing the value of LL is attributed to the reduction of the soil's affinity for water, resulting in a decrease in the diffuse double layer. However, the PL was increased at the 0.6% content of nano-SiO_2 by 12.5%. The increase in PL is attributed to the attraction of the negative surface of clay minerals to the cations. Subsequently, the PI is decreased. The reduction of PI was of the order of 53%. Beyond that content, the LL and PI were increased. The consistent outcomes were reported by Changizi and Haddad [6]. They observed that the LL decreased by 11.5%, the PL increased by approximately 13% and the PI declined by 52% at the optimum content of 0.7% of nano-silica.

5.3. Mechanical properties

Test unconfined compressive strength (UCS) of soil-nano-silica samples with different percentages and curing times are demonstrated in Figures 9-11. The UCS of the soft soil was 77kPa. Incorporation of 0.6%, 1.2%, 1.8%, 2.4% and 3% of nano-silica increased the UCS to 237.6kPa, 260 kPa, 288 kPa, 296.6 kPa and 334 kPa, corresponding to 208.575, 237.665, 274.035, 285.19% and 333.77% improvement, respectively, after 1day curing. Addition of 0.6%, 1.2%, 1.8%, 2.4% and 3% of nano-silica raised the UCS from 98.8kPa of untreated soil sample to 279kPa, 263kPa, 245kPa, 368kPa and 344kPa, corresponding to 182.39%, 166.19%, 147.98%, and 272.47% and 248.18% improvement, respectively, after 7days curing. Introduction of 0.6%, 1.2%, 1.8%, 2.4% and 3% of nano-silica increased the UCS from 140kPa of untreated soil sample to 461kPa, 422.5kPa, 502kPa, 492kPa and 460kPa, corresponding to 184.38%, 84.97%, 110.27%, 128.67% and 109.49% improvement, respectively, after 28days curing. Nano-silica significantly reduced strain at failure, consistent with previous findings [6, 8, 11]. Figure 11 presents the elastic modulus E50 of soil specimens containing different percentages of nano-silica (0%, 0.6%, 1.2%, 1.8%, 2.4% and 3%) at curing periods of 1day, 7days, and 28days. It can be seen that, the increase of E50 are 181.74-108.75 88.41%, 263.64-96.78-87.58%, 302.8-

106.23-113.25%, 285.2-209.76-131.9% and 306.66-117.17-112.46%, respectively, after 1-7-28days curing. Figure 12 shows the failure characteristics of soil specimens with different percentages of nano-silica after 28 days of curing. The soft soil specimen exhibited plastic failure, with minor cracks initiating under loading (Figure 12a). In contrast, specimens treated with nano-silica demonstrated brittle behavior (Figure12b and c). At higher contents, the failure became more brittle, producing sharper shear planes and blocky disintegration (Figure 12d, e and f).

5.4. Permeability Characteristics

Figure 14 illustrates the variation of the permeability coefficient of soil specimens with 0%, 0.6%, 1.8%, and 3% of nano-silica at curing periods of 1day, 7days, and 28days. The incorporation of nano-silica significantly reduced permeability, with reductions of 66.2-100%, 61.6-86.9%, and 53.8-81.8%. A sharp reduction in permeability was observed at 0.6% of nano-silica. Afterwards, a linear relationship between coefficient of permeability and nano-silica were observed. This behavior is attributed to the catalytic role of nano-SiO_2 (CAS No. 112945-52-5), which accelerates hydration reactions densifies the soil matrix (Figure 15b).

5.5. Microstructural analysis and Pore Size Distribution

Figure 14 shows FESEM images of soil specimens with 0%, 0.6%, and 3% nano-silica. The soft soil displays a loose, fibrous structure with rod-like clay particles, visible voids, and weak contacts (Figure 14a). At 0.6% nano-silica, particles are densely packed as silica nanoparticles fill pores and form bridges (Figure 14b). The pozzolanic reaction produces C-S-H gels that refine voids and enhance strength and stiffness. At 3% nano-silica (Figure 14c), excessive C-S-H clustering causes agglomeration, larger pores consequently decrease strength, elastic modulus and increases LL, PI and permeability. Figure 15 presents pore size distribution histograms. The soft soil specimen has an average pore diameter of 36.5 nm and porosity of 44%, reflecting poor bonding and low strength (Figure 15a). At 0.6% nano-silica, the average pore diameter and porosity decrease to 24.7 nm and 10%, representing a 32% reduction in void ratio. The bell-shaped curve indicates refined voids and uniform C-S-H gel formation (Figure 15b). At 3% nano-silica, the average pore diameter increases to 37.7 nm and porosity to 25%, showing 3% pore growth (Figure 15c). The irregular curve reflects heterogeneous clustering and micro-cracks, explaining the decline in UCS and E50 beyond the optimum content. Maximum stiffness is achieved at 0.6% nano-silica, where void refinement and uniform gel distribution balance the engineering properties of the soil.

5.6. Repeatability and Reproducibility

5.6.1. Index properties

Standard deviation error bars for $\boldsymbol{G_s}$ highlight the consistency of results across nano-silica dosages. Narrow bars confirm strong repeatability with limited random error, while the steady increase in $\boldsymbol{G_s}$ demonstrates reproducibility of the treatment effect. This validates both measurement precision and the reliability of nano-silica enhancement (Figure 16a).Error bars reveal stable LL and PL values with strong repeatability, while PI shows greater variability due to its dependence on both limits. Even with this dispersion, the consistent pattern of lower LL, slightly higher PL, and reduced PI confirms reproducibility, proving that nano-silica reliably alters soil consistency (Figure 16b).

5.6.2. Mechanical properties

Figures 11 and 17 illustrate the standard deviation error bars of the reliability of UCS and E50 measurements. At 0.6% nano-silica, the tight scatter confirms optimal repeatability, whereas higher dosages (≥2.4%) exhibit larger deviations due to particle agglomeration, heterogeneous dispersion, and localized reaction variability. The progressive reduction in scatter with curing time demonstrates that extended pozzolanic activity enhances both repeatability and reproducibility of strength and elastic modulus improvements.

5.6.3. Permeability Characteristics

Error bar analysis confirms that the reduction in permeability with nano-silica is consistent and reproducible, not just evident in mean values. Wider scatter at early curing stages reflects sensitivity to nanoparticle dispersion, but the overall trend of improved hydraulic resistance remains reliable, demonstrating acceptable repeatability and strong reproducibility (Figure 18).

5.7. Limitations of this study

It should be noted that the results of specific gravity ($\boldsymbol{G_s}$) and Atterberg limits were obtained after 1-day of curing only, without consideration of longer curing periods, such as 7 or 28 days. This represents a limitation, as extended curing may influence soil consistency and microstructural interactions, thereby affecting the reliability of these parameters. Moreover, the tests were conducted under constant laboratory conditions; variations in temperature, pH, and clay percentage could alter the behavior of MH soils treated with nano-silica. Therefore, future studies should examine different soil types and environmental conditions and extend the work to field-scale prototypes to validate practical applicability.

6. Conclusion

The novelty of the present work lies in compacting MH specimens on the wet side of the OMC point, systematically evaluating their engineering properties and microstructural outcomes, and pore size distribution using the FESEM, which are rarely used in soil stabilization. This work showed that compacting soil specimens with nano-silica on the wet-side of OMC by remolding device significantly enhanced the geotechnical properties. The effects were investigated through a series of results provided from $\boldsymbol{G_s}$, Atterberg limit, UCS, E_{50} and permeability. Nanomaterials can enhance the performance of MH soils in various civil engineering applications. Nano-silica shows great potential for use in foundation construction, dam cores, landfill linings, roadbeds, and earthworks. Additionally, nano-silica can be used in the manufacture of building bricks. The following conclusions were limited to MH soil, and the experiments were conducted under controlled laboratory conditions without field verification:

1. The Addition of nano-silica increases $\boldsymbol{G_s}$ monotonically.
2. The addition of nano-silica decreases PI by 53% at 0.6%. Beyond that percentage, the PI initiates an increase.
3. UCS for soil specimens, incorporating 0.6%, 1.2%, 1.8%, 2.4%, and 3% of nano-silica, were increased by 208.6%, 237.7%, 274.0%, 285.2% and 333.8%, respectively, after 1 day of curing.
4. UCS for soil specimens, introducing 0.6%, 1.2%, 1.8%, 2.4%, and 3% of nano-silica, were increased by 182.4%, 166.2%, 148.0%, and 272.5% and 248.2%, respectively, after 7 days of curing.
5. UCS for soil specimens, adding 0.6%, 1.2%, 1.8%, 2.4%, and 3% of nano-silica, were increased by 184.4%, 85.0%, 110.3%, 128.7%, and 109.5%, respectively, after 28 days of curing.
6. The results showed that nano-silica has a positive impact on the elastic modulus of specimens. Addition of nano-silica reduces the failure strain.
7. The reduction in coefficient of permeability for specimens, introducing 0.6%, 1.8%, and 3% at different curing times (1 day, 7 days, and 28 days), ranged between 66.2-100%, 61.6-86.9%, and 53.8-81.8%.
8. FESEM and pore size analyses confirmed that nano-silica significantly refines soil microstructure. At 0.6% content, voids were improved, porosity reduced by 32%, and strength enhanced due to uniform C–S–H gel distribution.
9. In contrast, 3% nano-silica caused agglomeration, larger pores, and reductions in UCS, modulus, and permeability.
10. The Standard deviation of error bars exhibits particle agglomeration, heterogeneous dispersion, and localized reaction variability.
11. Standard deviation of error bars confirms the reliability, repeatability, and reproducibility of test results.
12. Based on results obtained from tests and microstructural analysis, the optimum content of nano-silica for MH soil is 0.6%.

Future works should include variation of environmental conditions, testing on diverse soil types and validation at field scale.

Acknowledgment

This experiment was carried out at the Soil and Rock Laboratory of the Civil Engineering Department of the Engineering College of Salahaddin University-Erbil, whose support is sincerely appreciated. Special thanks are extended to Erbil Construction Laboratory for the procurement of Dwin soft soil and for performing chemical composition analysis free of charge.

References

[1] Khalid, N., M. Mukri, F. Kamarudin, and A.H. Abdul Ghani. *Effect of compaction characteristics on hydraulic conductivity performance for sedimentary residual soil mixed bentonite as compacted liners*. in *IOP Conference Series: Earth and Environmental Science*. 2020. IOP Publishing.

[2] Mir, B. and S. Reddy, *Mechanical behaviour of nano-material (Al2O3) stabilized soft soil.* International Journal of Engineering, 2021. **34**(3): p. 636-643.

[3] Diana, W., E. Hartono, and A. Muntohar. *The permeability of Portland cement-stabilized clay shale*. in *IOP Conference Series: Materials Science and Engineering*. 2019. IOP Publishing.

[4] Yacine, D.M., D. Mehdi, M. Zakaria, and G. Aboubakar, *Experimental Analyses of the Effect of Polypropylene Fibers on Consistency Limits and Permeability of Clays.* Studies in Science of Science| ISSN: 1003-2053, 2024. **42**(9): p. 77-88.

[5] Changizi, F. and A. Haddad, *Strength properties of soft clay treated with mixture of nano-SiO2 and recycled polyester fiber.* Journal of rock mechanics and Geotechnical Engineering, 2015. **7**(4): p. 367-378.

[6] Changizi, F. and A. Haddad, *Improving the geotechnical properties of soft clay with nano-silica particles.* Proceedings of the Institution of Civil Engineers-Ground Improvement, 2017. **170**(2): p. 62-71.

[7] Kalhor, A., M. Ghazavi, and M. Roustaei, *Impacts of nano-silica on physical properties and shear strength of clayey soil.* Arabian Journal for Science and Engineering, 2022. **47**(4): p. 5271-5279.

[8] Abd, K.G. and A.H. Abd, *Effect of Waterproofed Nano-silica on Some Engineering Properties of Gypseous Soil.* Tikrit Journal of Engineering Sciences, 2025. **32**(4): p. 1-11.

[9] Gu, J., et al., *Evaluating the effect of nano-SiO2 on different types of soils: a multi-scale study.* International Journal of Environmental Research and Public Health, 2022. **19**(24): p. 16805.

[10] Lu, J., et al., *Improved mechanical behaviour and microstructure of cemented soil with nanomaterials.* KSCE Journal of Civil Engineering, 2024. **28**(7): p. 2738-2749.

[11] Chen, Z., et al., *Sustainable soil stabilization with Nano-Silica and polypropylene fibers mechanical properties durability and microstructural analysis.* Scientific Reports, 2026.

[12] Wang, S., et al. *Effects of Leachate Concentration (Na+, Pb2+, COD) on Non-Darcy Flow of Compacted Clay*. in *The International Congress on Environmental Geotechnics*. 2018. Springer.

[13] Özçoban, M.Ş. and S. Acarer, *Investigation of the effect of leachate on permeability and heavy metal removal in soils improved with nano additives.* Applied Sciences, 2022. **12**(12): p. 6104.

[14] Matos, M.P., A.A.S. Correia, and M.G. Rasteiro, *Application of carbon nanotubes to immobilize heavy metals in contaminated soils.* Journal of Nanoparticle Research, 2017. **19**(4): p. 126.

[15] Mohammadi, M., M. Khodaparast, and A.M. Rajabi, *Effect of nano calcium carbonate (nano CaCO3) on the strength and consolidation properties of clayey sand soil.* Road Materials and Pavement Design, 2022. **23**(10): p. 2394-2415.

[16] Choobbasti, A.J. and M. Valizadeh, *The effect of nano-CuO on mechanical, microstructural, and self-healing properties of clayey sandy soils.* Arabian Journal of Geosciences, 2022. **15**(15): p. 1346.

[17] Karumanchi, M., G. Avula, R. Pangi, and S. Sirigiri, *Improvement of consistency limits, specific gravities, and permeability characteristics of soft soil with nanomaterial: Nanoclay.* Materials Today: Proceedings, 2020. **33**: p. 232-238.

[18] Kannan, G., E.R. Sujatha, and B.C. O'Kelly, *Investigation on geoengineering properties of organic silt soil treated with chitosan nanoparticle additive.* Scientific Reports, 2026.

[19] Esmaeili, N., et al., *Evaluating the environmental-friendly stabilization of loess soil with nano iron oxide: enhanced strength and non-destructive monitoring through UPV.* International Journal of Environmental Science and Technology, 2026. **23**(3): p. 176.

[20] Barimani, M., H. Motaghedi, S. Soleimani Kutanaei, and A. Ebrahimi, *Stabilizing collapsible soils using nano calcium carbonate to enhance mechanical properties.* Scientific Reports, 2026.

[21] Solórzano-Blacio, C. and J. Albuja-Sánchez, *Effect of nanosilica on the undrained shear strength of organic soil.* Nanomaterials, 2025. **15**(9): p. 702.

[22] Chen, S., X. Ou, J. Jiang, and Z. Tan, *Experimental Study on the curing mechanism of red mud-based stabilized soil co-modified by Nano-SiO2 and gypsum.* Materials, 2023. **16**(17): p. 6016.

[23] Al-Khazzaz, Z., A. Aldaood, M. Awad, and M.K. Faris, *Behavior of clayey soil treated with nano magnesium oxide material.* Soils and Rocks, 2024. **47**(1): p. e2024014822.

[24] Murthy, V., *Advanced foundation engineering*. 2007: CBS publishers & distributors Chennai.

[25] Look, B.G., *Handbook of geotechnical investigation and design tables*. 2007: Taylor & Francis.

تأثير السيليكا النانوية على الخصائص الجيوتقنية والتحليل الميكروي للتربة اللينة

المستخلص

تُقدِّم تقنية النانو نهجًا مبتكرًا لتثبيت التربة في الهندسة الجيوتقنية. تتناول هذه الدراسة الخصائص الفيزيائية والميكانيكية والهيدروليكية للتربة المُعالجة بجزيئات السيليكا النانوية بنسب ٠٪، ٠.٦٪، ١.٢٪، ١.٨٪، ٢.٤٪، و٣٪. تمّ ضغط عينات التربة لاختبار مقاومة الضغط غير المحصور (UCS) والنفاذية باستخدام جهاز إعادة التشكيل. تكمن حداثة هذه الدراسة في ضغط الطين عالي اللدونة (MH) بنسبة ٩٥٪ من أقصى كثافة جافة على الجانب الرطب من محتوى الرطوبة الأمثل (OMC)، المُحدد من اختبار بروكتر القياسي لضغط التربة غير المُعالجة. أدى إدخال ٠.٦٪ من جزيئات السيليكا النانوية إلى خفض حد السيولة (LL) ومؤشر اللدونة (PI) بنسبة ١٣٪ و٥٣٪ على التوالي. عند فترات معالجة مدتها يوم واحد، وسبعة أيام، وثمانية وعشرين يوماً، زادت مقاومة الضغط غير المحصور ومعامل المرونة (E50) بنسبة ٢٠٨٪–١٨١.٧٤٪، و١٨٢.٣٩٪–١٠٨.٧٥٪، و١٨٤.٣٨٪–١٨٨.٤١٪ على التوالي، عند استخدام ٠.٦٪ من السيليكا النانوية. علاوة على ذلك، لوحظ انخفاض حاد في النفاذية عند نسبة ٠.٦٪، تلاه ارتفاع خطي عند النسب الأعلى. أكد تحليل المجهر الإلكتروني الماسح ذي الانبعاث الميداني (FESEM) إعادة ترتيب الجسيمات وتكوين الهلام، مما أدى إلى تحسين المسام وزيادة المتانة. كما انخفض متوسط قطر المسام بنسبة ٣٢٪ تقريباً مع إضافة ٠.٦٪ من السيليكا النانوية. مع ذلك، تسببت الكمية الزائدة من السيليكا النانوية في التكتل، مما أدى إلى خصائص هندسية غير مرغوبة.

الكلمات المفتاحية:

التربة الرخوة؛ السيليكا النانوية؛ تحسين التربة؛ الخصائص الجيوتقنية؛ التحليل الميكروي.

Figure 1. Location of the study area.

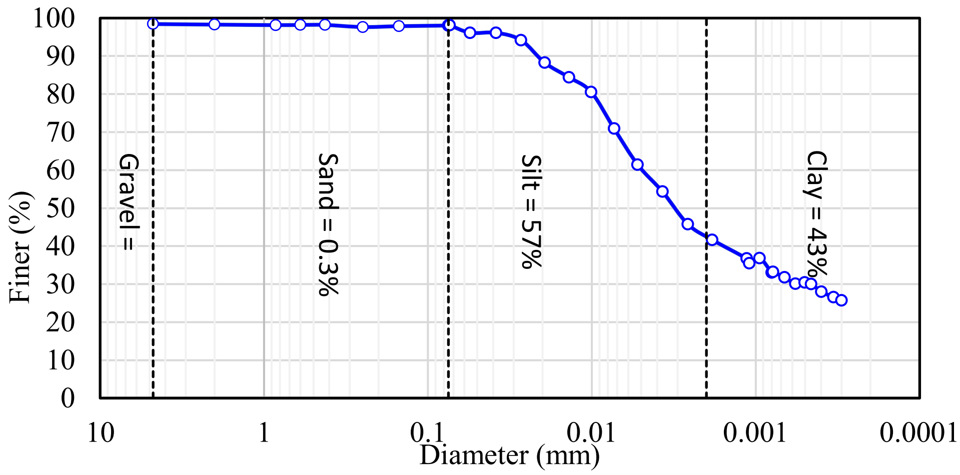

Figure 2. Particle size distribution of Dwin soil.

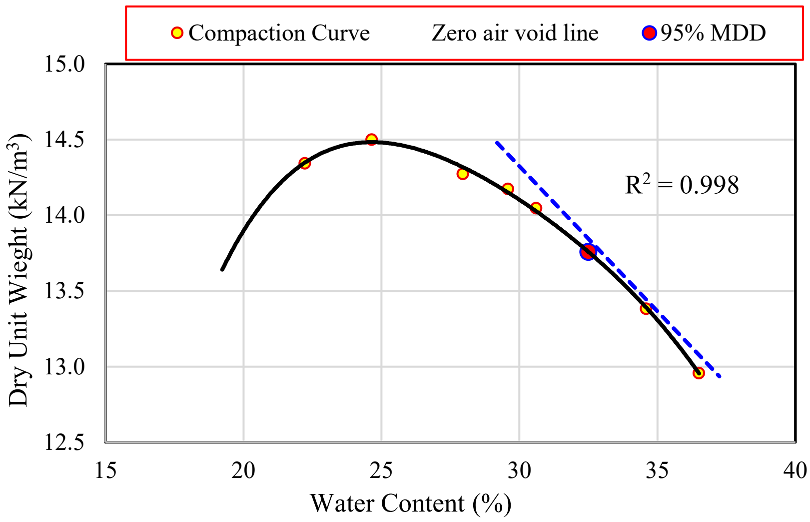

Figure 3. Standard proctor compaction curve of Dwin soil sample.

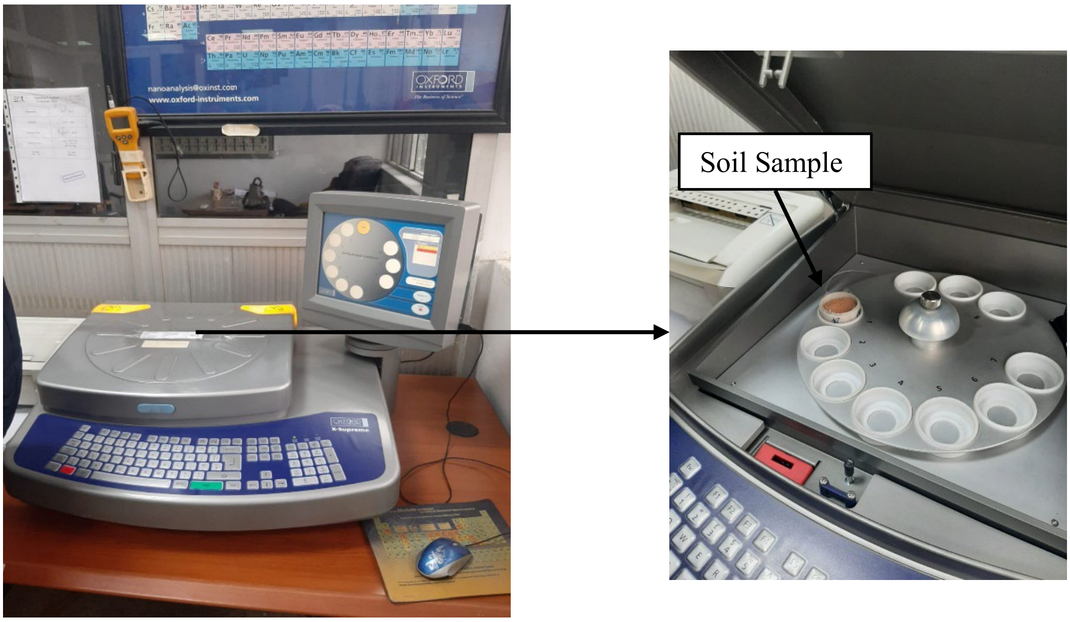

Figure 4. Preparation of chemical composition analysis using XRF spectrometer device.

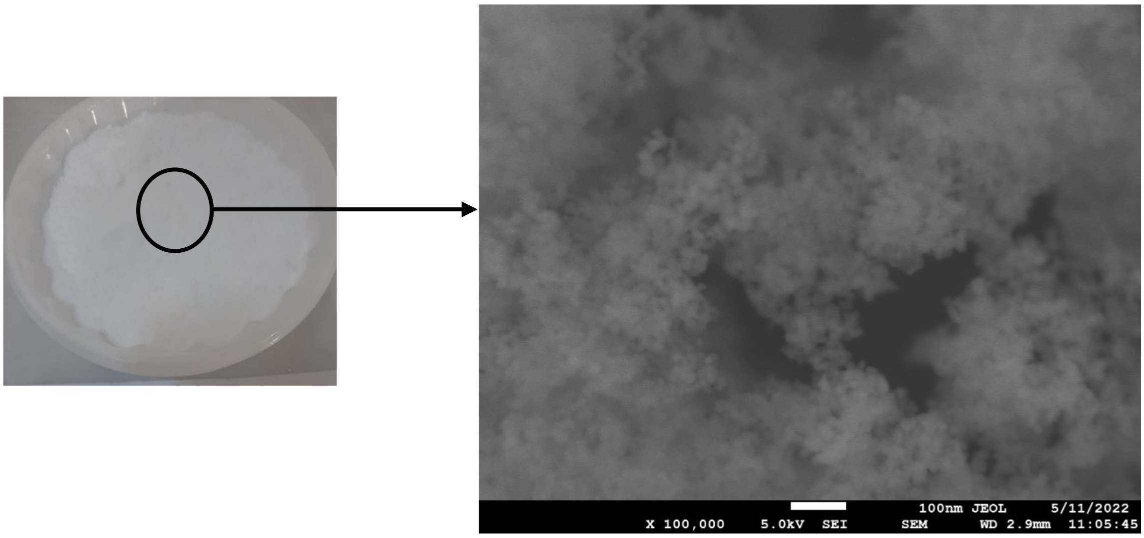

Figure 5. Illustration of Nano silica appearance as white dry powder and SEM image of nanoparticles.

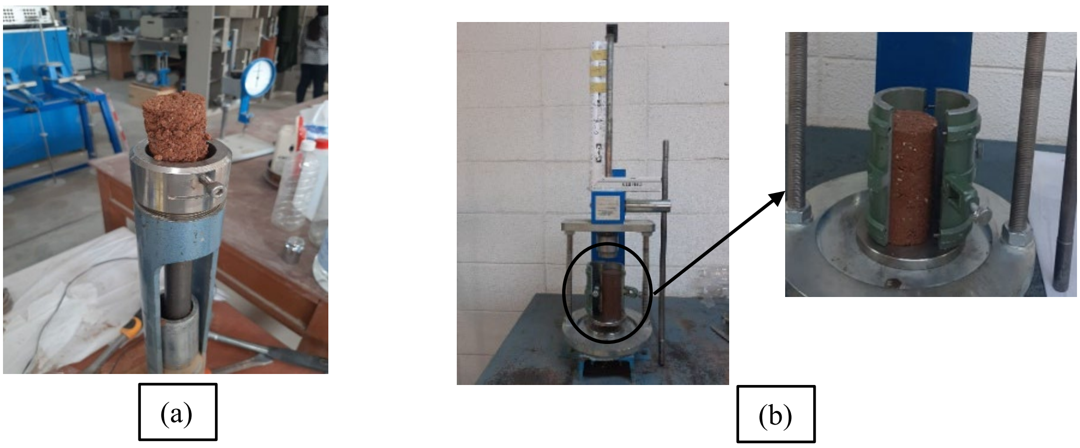

Figure 6. a) Deterioration of soft soil sample when it was compacted in a rigid mold. b) Compacting soft soil sample in a separate mold without deterioration by remolding device.

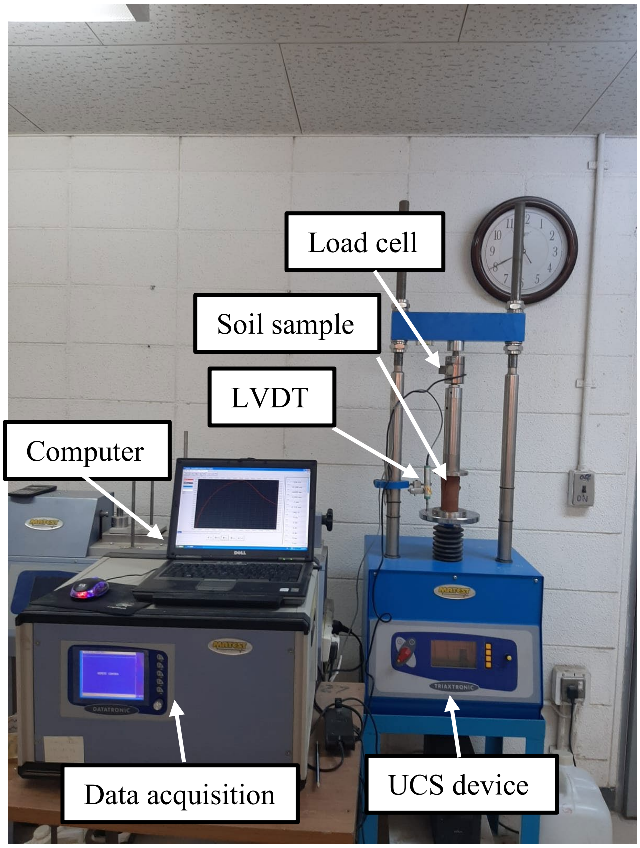

Figure 7. Laboratory setup for unconfined compressive strength (UCS) testing of soil–nano-silica specimens.

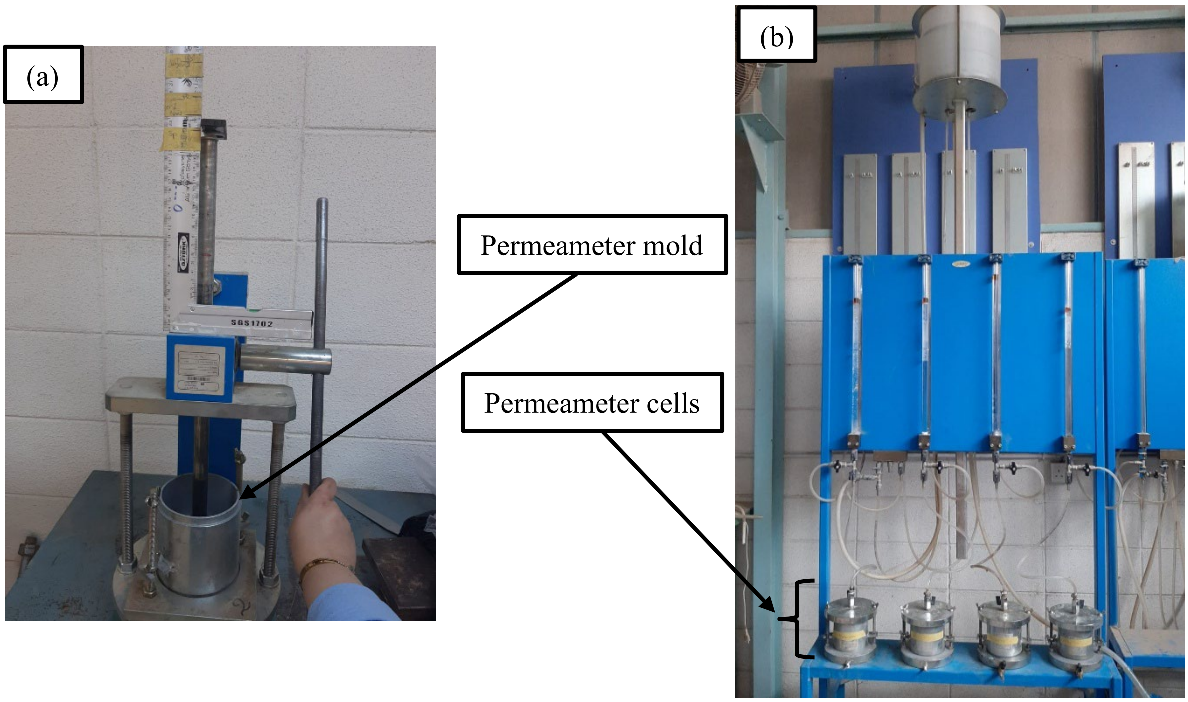

Figure 8. a) Compacting the soil samples at its target density and water content by remolding device. b) Falling head permeability testing system.

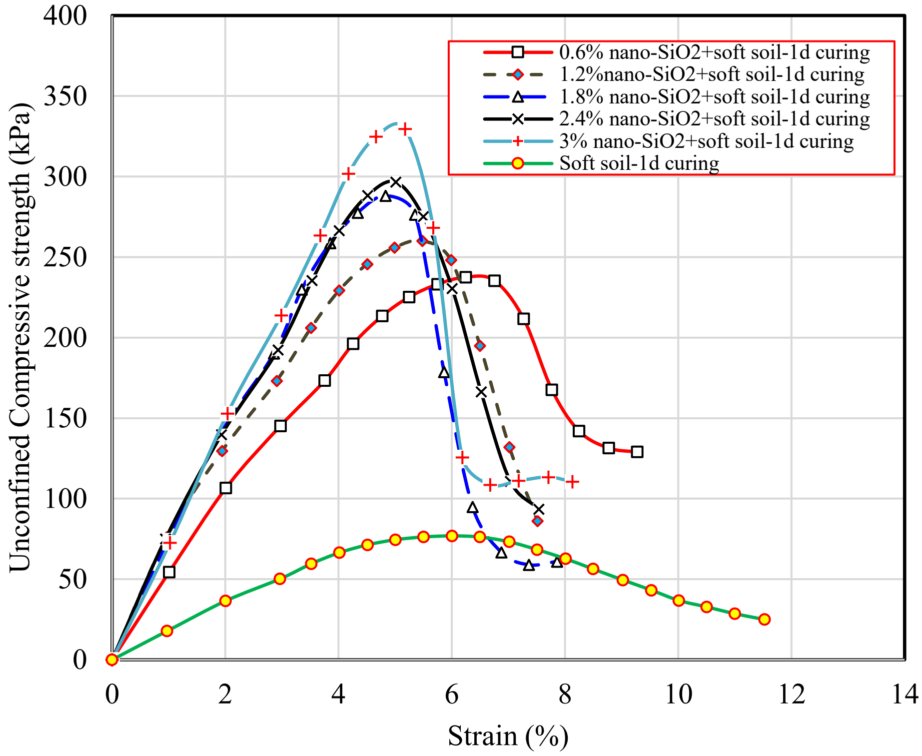

Figure 9. The unconfined compressive strength UCS of soil-nano-silica samples at different percentages of nano-silica (0, 0.6, 1.2, 1.8, 2.4 and 3%) after 1day curing.

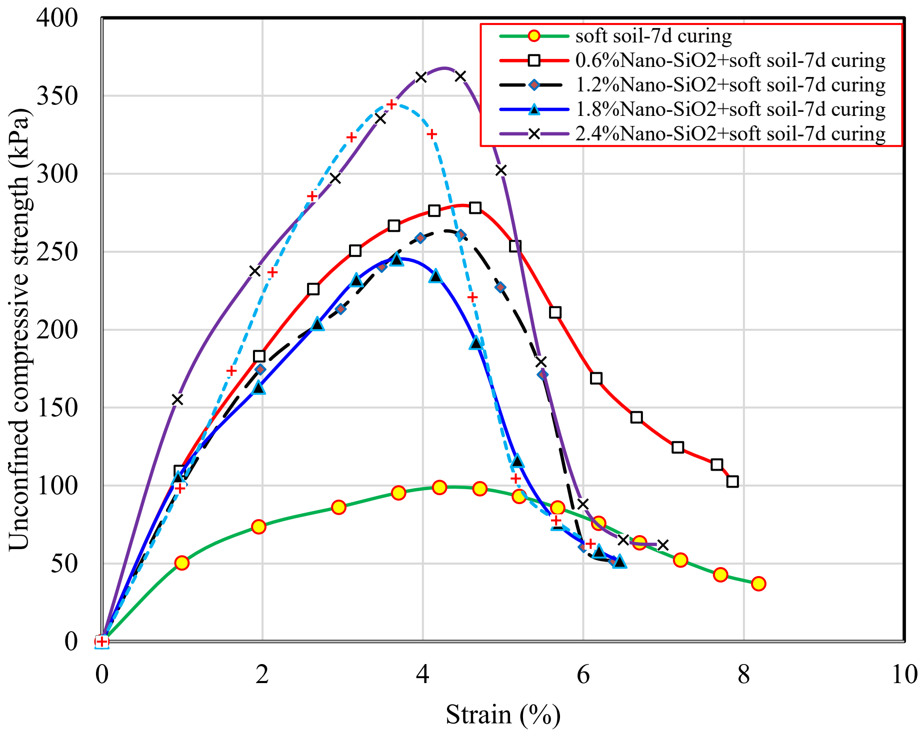

Figure 10. The unconfined compressive strength UCS of soil-nano-silica samples at different percentages of nano-silica (0, 0.6, 1.2, 1.8, 2.4 and 3%) after 7days curing.

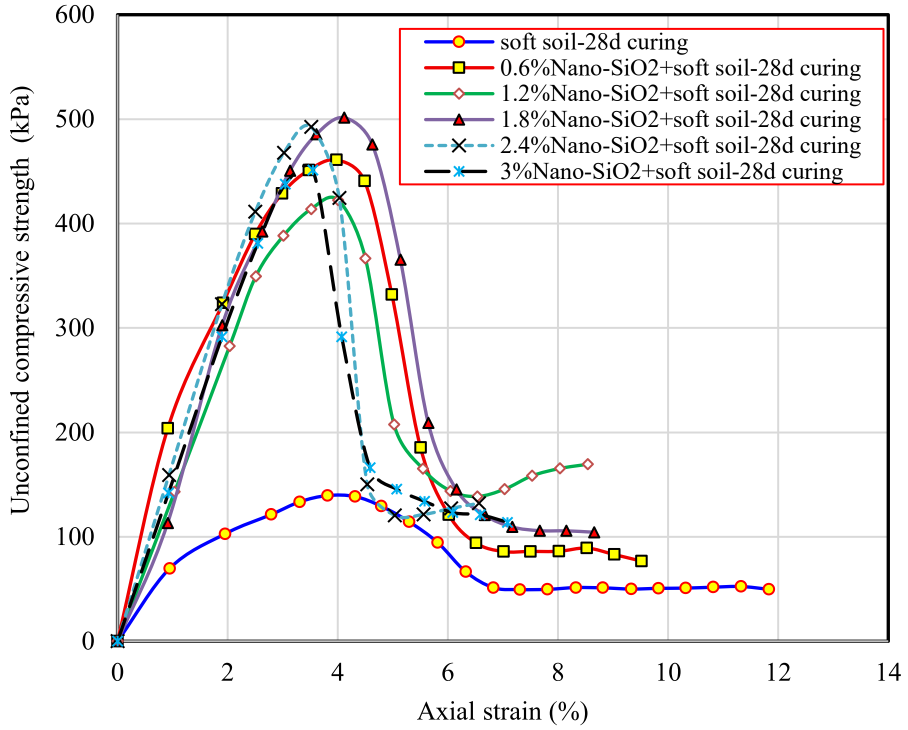

Figure 10. The unconfined compressive strength UCS of soil-nano-silica samples at different percentages of nano-silica (0, 0.6, 1.2, 1.8, 2.4 and 3%) after 28 days curing.

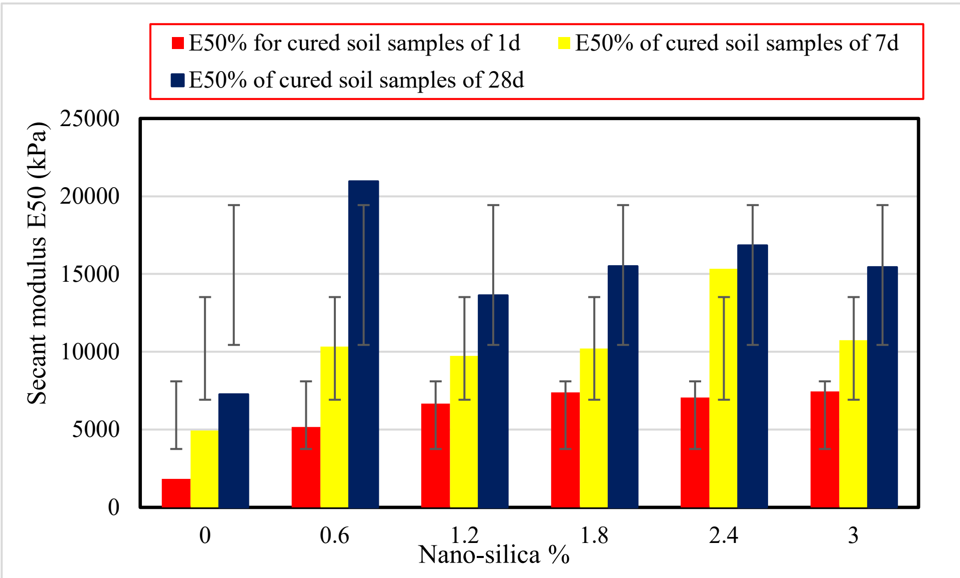

Figure 11. Secant modulus E_{50} of soil-nano-silica samples at different percentages of nano-silica (0, 0.6, 1.2, 1.8, 2.4 and 3%) and curing time (1, 7 and 28days), with error bars representing standard deviation.

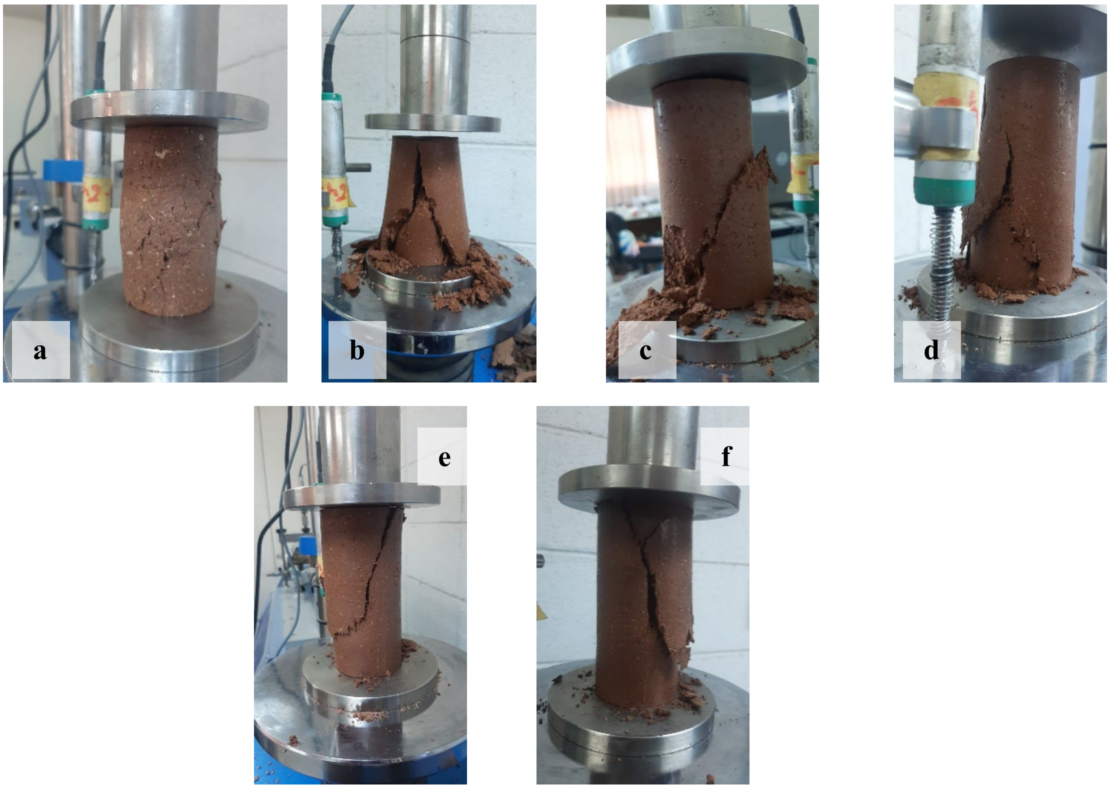

Figure 12. Effect of nano-silica on failure characteristics of soil specimens after 28 days curing: a) soft soil; b) soil-nano-silica specimen at 0.6% of nano-silica; c) soil-nano-silica specimen at 1.2% of nano-silica; d) soil-nano-silica specimen at 1.8% of nano-silica; e) soil-nano-silica specimen at 2.4% of nano-silica and f) soil-nano-silica specimen at 3% of nano-silica.

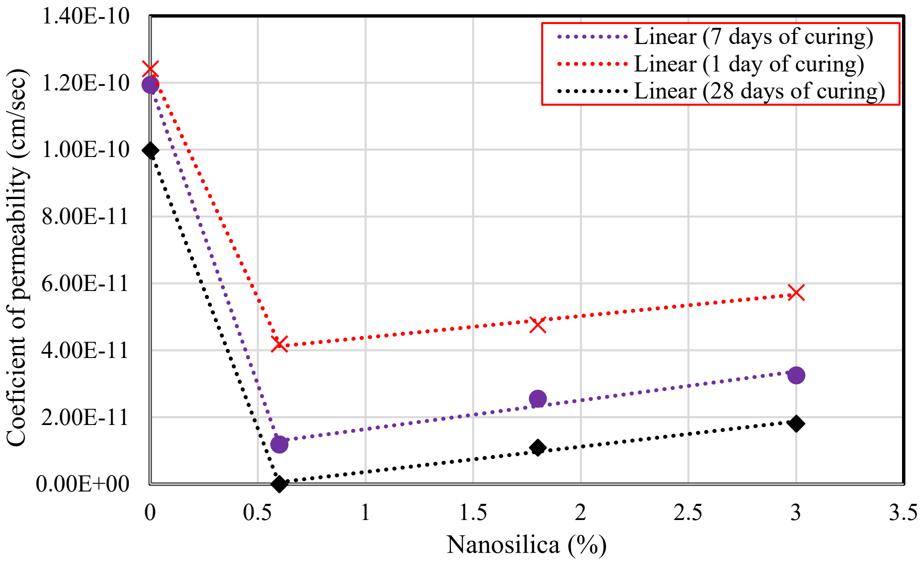

Figure 13. The coefficient of permeability soil-nano-silica samples at various percentages of nano-silica (0.6, 1.8 and 3%) and curing time (1, 7 and 28days), with error bars representing standard deviation.

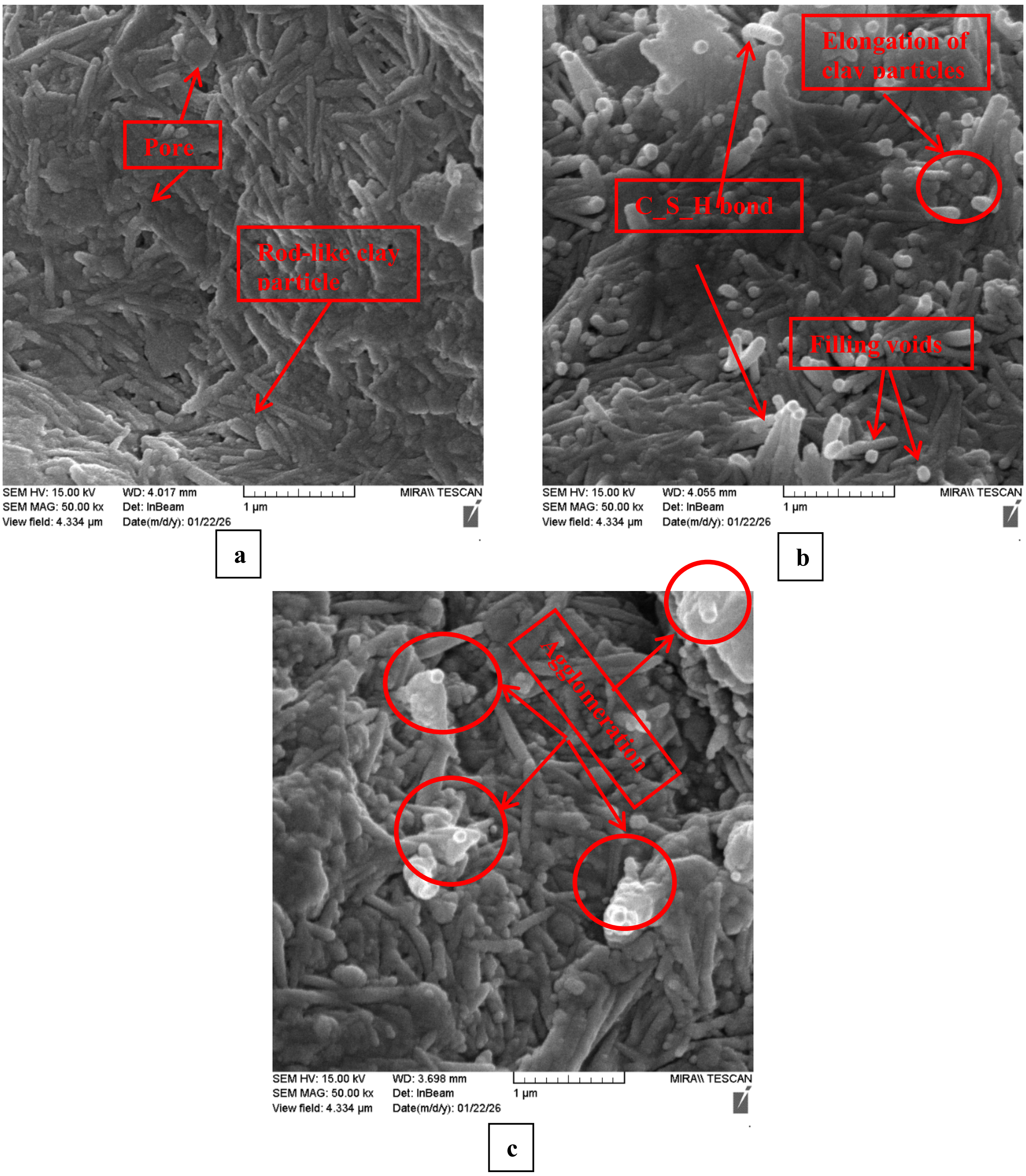

Figure 14. Illustration of FESEM images of failed samples at 28 days curing: a) Soft soil, b) Soil-nano-silica at the percentage of 0.6% and c) Soil-nano-silica at the percentage of 3%.

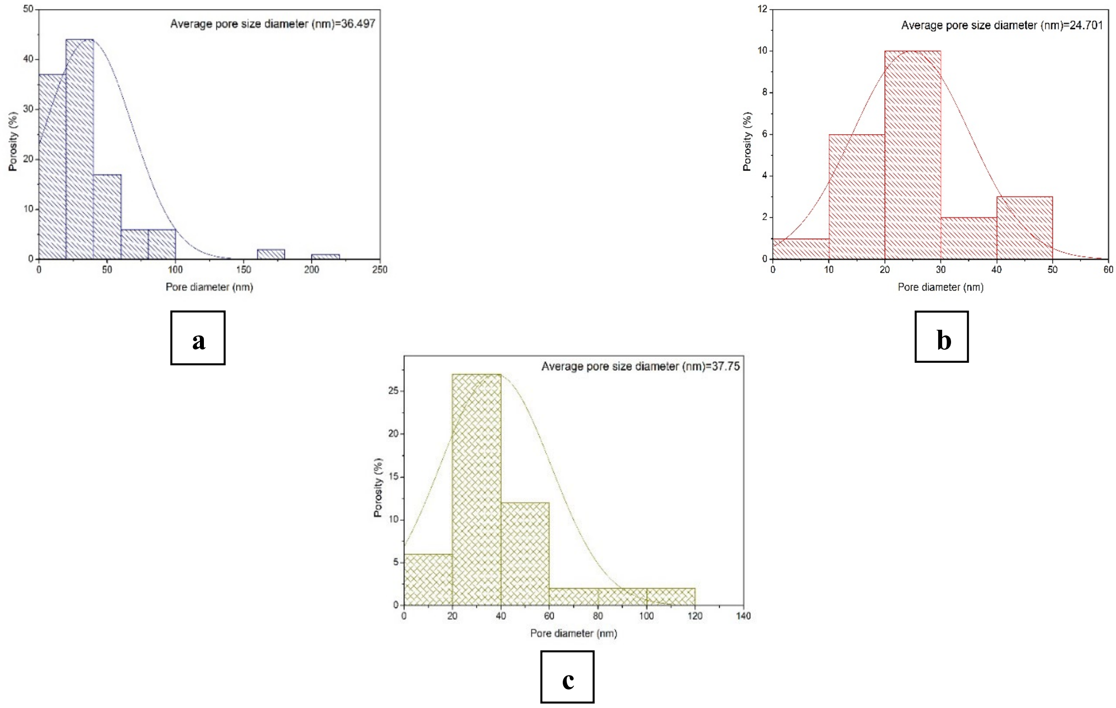

Figure 15. Pore size distribution derived from FESEM analysis at 1 µm of failed samples after 28days curing: a) untreated soft soil, b) soil-nano-silica stabilized with 0.6% nano-silica and c) soil-nano-silica stabilized with 3% nano-silica.

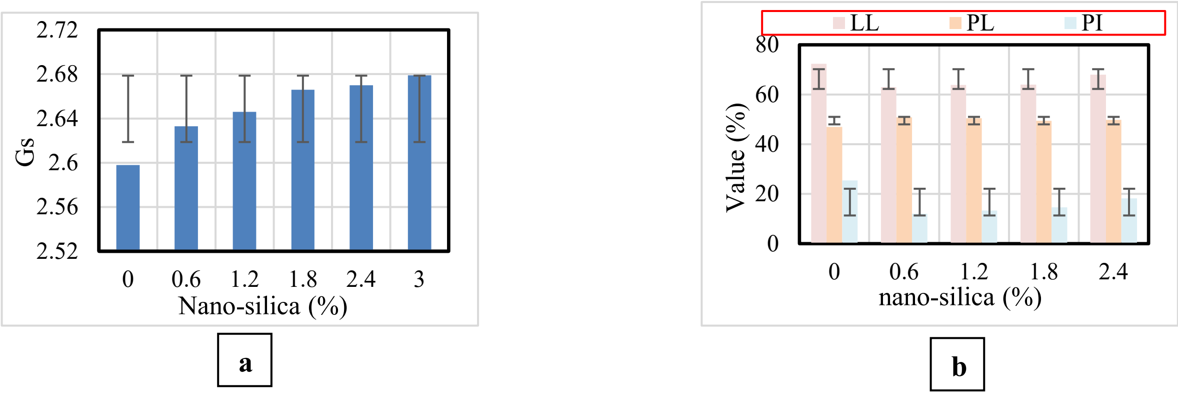

Figure 16. Error bars (standard deviation) for different percentages of nano-silica (0%, 0.6%, 1.2%, 1.8%, 2.4% and 3%) of: a) Gs. b) LL, PL and PI.

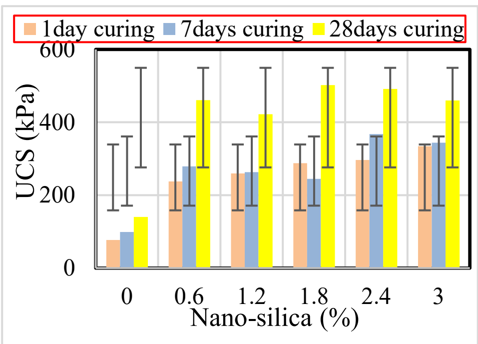

Figure 17. Error bars (standard deviation) of Unconfined Compressive Strength (UCS) for different percentages of nano-silica (0%, 0.6%, 1.2%, 1.8%, 2.4% and 3%) and curing times (1, 7, and 28 days).

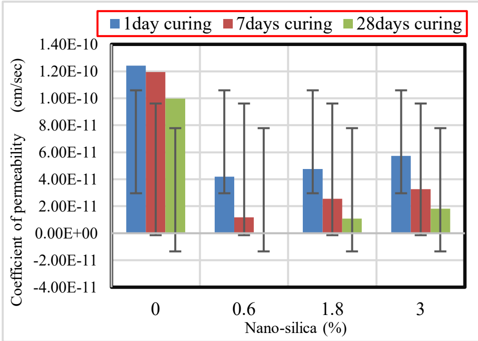

Figure 18. Error bars (standard deviation) of coefficient of permeability for different percentages of nano-silica (0%, 0.6%, 1.2%, 1.8%, 2.4% and 3%) and curing times (1, 7, and 28 days).

Table 1. The results of chemical composition of Dwin soil analysis using XRF spectrometer.

Chemical Composition	**Concentration (%)**
SiO_2	28.32
CaO	18.67
Fe_2O_3	5.467
Al_2O_3	1.761
MgO	1.4229
SO_3	1.04
P_2O_5	0.4421
TiO_2	0.2699
Na_2O	0.26686
Mn_2O_3	0.096
K_2O	0.0797

Wt: weight percent (also called mass percent).

Table 2. The result of Specific gravity G_s of the soil-nano-silica samples at different percentages of nano-silica (0, 0.6, 1.2, 1.8, 2.4 and 3%).

Nano-SiO_2 (%)	**G_s Value**
0	2.598
0.6	2.633
1.2	2.646
1.8	2.666
2.4	2.67
3	2.679

Table 3. The results of LL, PL and PI and plasticity of soil-nano-silica samples at different percentages of nano-silica. (0, 0.6, 1.2, 1.8, 2.4 and 3%).

Nano-SiO_2 (%)	**Liquid limit (%)**	**Plastic limit (%)**	**Plastic index (%)**	**Plasticity [24]**
0	72.4	47	25.4	High plastic
0.6	62.9	50.87	12.03	Moderate plastic
1.2	63.8	50.46	13.34	
1.8	64	49.43	14.57	
2.4	68	49.76	18.24	High plastic
3	69.6	48.11	21.49	

Table 4. Soil strength classification of silt-dominant MH soil according secant modulus E_{50} [25].

Soil type	**Soil consistency**	**E_{50} (kPa)**
		Short term
Silt	Soft	<10000
	Stiff	10000-20000
	Hard	>20000